forests

MDPI

Article

Hydraulics Facilitate Urban Forest Establishment by Informing Tree Dynamics under Drought

Ye Wang [1], Ting Liao [1], Liqin Guo [1], Guobin Liu [1,*] and Benye Xi [2]

[1] Institute of Forestry and Pomology, Beijing Academy of Agriculture and Forestry Sciences, 12 A Rui Wang Fen, Fragrance Hills, Haidian District, Beijing 100093, China; wangye@baafs.net.cn (Y.W.); liaoting@baafs.net.cn (T.L.); guoliqin@baafs.net.cn (L.G.)

[2] Key Laboratory for Silviculture and Conservation of Ministry of Education, Beijing Forestry University, Beijing 100083, China; benyexi@bjfu.edu.cn

* Correspondence: liuguobin@baafs.net.cn; Tel.: +86-10-6267-3627

Abstract: Urban forests provide considerable ecosystem services for city dwellers, yet the function of forest species is increasingly challenged by urban drought. Understanding drought tolerance of urban forest species would facilitate vegetation conservation and establishment within urban ecosystems. Here, we report on the drought resistance of leaves for two exotic and three indigenous tree species common to the Jing-Jin-Ji metropolitan region (covering Beijing, Tianjin, and Hebei province) of north China. Xylem vulnerability to drought-induced embolism and leaf gas exchange, together with various morphological and anatomical traits that potentially relate to plant water use, were measured for pot-grown seedlings. In addition, seedlings were subjected to dry-down at two different drought intensities until death, and the tree mortality rate was recorded. We found that species differ markedly in xylem embolism resistance, with indigenous species showing more negative P_{50} (the water potential triggering 50% loss of xylem hydraulic conductivity), but less canopy leaf area at a given branch basal diameter, compared with exotic species. Furthermore, P_{50} well predicted tree mortality rate under protracted drought stress. Species characterized by more negative P_{50} also exhibited higher maximum leaf photosynthetic rates. In addition, leaf P_{50} was found to correlate with specific leaf area, while the hydraulic safety margin was related to sapwood density and the thickness of the leaf upper epidermis. Collectively, these results highlight the role of embolism resistance in dictating drought response and the promise of morphological traits as proxies of plant physiological drought resistance. Our findings contribute to understanding drought response for urban tree species and will guide the establishment and management of urban forests.

Keywords: urban forests; drought; water relation; embolism resistance; gas exchange; tree mortality

check for updates

Citation: Wang, Y.; Liao, T.; Guo, L.; Liu, G.; Xi, B. Hydraulics Facilitate Urban Forest Establishment by Informing Tree Dynamics under Drought. *Forests* **2023**, *14*, 2415. https://doi.org/10.3390/f14122415

Received: 26 October 2023
Revised: 11 November 2023
Accepted: 13 November 2023
Published: 12 December 2023

Copyright: © 2023 by the authors. Licensee MDPI, Basel, Switzerland. This article is an open access article distributed under the terms and conditions of the Creative Commons Attribution (CC BY) license (https://creativecommons.org/licenses/by/4.0/).

1. Introduction

Climate change is expected to alter the global surface hydrological cycle, resulting in more frequent, long-lasting, and severe drought stress that challenges the health and function of vegetation in terrestrial ecosystems [1,2]. Such adverse effect is particularly evident in urban ecosystems, which account for only ca. 3% of land surface area but accommodate more than half of the global population [3], given that human settlements can often intensify the magnitude of drought by shifting the amount of precipitation or surface runoff, increasing water demand or by polluting water of both surface and belowground [4]. Plants living in urban ecosystems, including those inhabiting cities, towns, or suburbs, are commonly referred to as urban forests, which represent a small portion of terrestrial vegetation coverage [5], but deliver substantial social, economic, or ecological benefits to human beings, such as carbon sequestration, reducing energy costs or increasing community resilience [6,7]. Nevertheless, ecosystem services provided by urban forests are increasingly compromised by drought stress [3,8–10]. A recent meta-analysis showed that more than half of the urban forest species' performance has been threatened by

drought, with the proportion projected to increase because of ongoing climate change and accelerated urbanization [3]. Within this context, understanding the impacts of drought on urban forests is essential to developing management strategies for urban trees and achieving the sustainable development goals of the United Nations [4].

From a physiological perspective, drought stress compromises species performance primarily by affecting water transport [11,12]. The cohesion-tension theory explaining water movement along the soil-plant-atmosphere continuum (SPAC) states that the water column in conduits of transpiring plants is under tension, which arises due to the water vapor gradient between plants and the atmosphere [13,14]. Such a mechanism enables the movement of water along SPAC and requires minimal metabolic energy input but entails a crucial tradeoff since water in the conduits is under metastable state and thus characterized by low stability [15]. During drought stress, the tensile force will increase, leading to the aspiration of air bubbles from gas-filled conduits to water-filled conduits through inner conduit pits (i.e., air seeding hypothesis). The air bubble can then expand if tension is not timely alleviated, ultimately forming air emboli that block the route of water transport (i.e., xylem embolism) [16–18], resulting in a decline in leaf gas exchange, canopy dieback, or even whole plant mortality [12,19,20]. Therefore, the capacity of plants to resist xylem embolism, typically quantified by the water potential triggering a 50% loss of xylem hydraulic conductivity (P_{50}), has been widely recognized as a core attribute governing species drought tolerance [21], community abundance [22], and geographical distribution [23–25]. Xylem embolism resistance has been intensively examined in the past decades, yet many of the P_{50} values are obtained for species of natural ecosystems [26], while the P_{50} of urban forests remains largely understudied [27–29]. Knowledge regarding the xylem embolism resistance of urban forest species will provide informative guidance to species screening, planting site selection, and species-specific water management regime development during the establishment of green infrastructure in urban ecosystems.

Species with high (i.e., more negative) P_{50} appear advantageous under water deficit conditions [30]. However, it is hypothesized that an increase in xylem embolism resistance can cause reduced water transport capacity because of the structural tradeoff at the conduit level. Indeed, xylem with more negative P_{50} often consists of conduits characterized by reduced diameter, small and few inner conduit pits and/or less porous pit membrane, all of which could restrict the spread of air emboli under tension but meanwhile undermine water movement [31,32]. Given the intimate link between hydraulic transport and gas exchange efficiency, species equipped with better embolism resistance are expected to show reduced carbon assimilation efficiency and in turn growth rate, which would weaken species competitiveness when moisture condition is optimal [33,34]. However, experimental evidence regarding the tradeoff between embolism resistance and carbon acquisition is variable [23,28,35], with some species exhibiting both high carbon assimilation capacity and xylem embolism resistance [23]. Such an "efficiency-safety" tradeoff largely dictates overall plant water regulation strategy, thus holding critical implications for the drought resistance and resilience of species, which are vital to the functioning of urban forests [36].

Unlike natural ecosystems, urban forests often comprise a large portion of species introduced from diverse habitats (i.e., exotic species), where the environmental conditions of provenance can be distinct from those of the locals [37]. Although the utilization of exotic species together with indigenous species has been a common approach for constructing urban forests worldwide, its rationality remains under debate. One of the core questions surrounding the controversy lies in adaptiveness, which argues that exotic species are less well adapted to the local environment where they are introduced and, hence, may be outperformed by indigenous species in terms of ecosystem services [38]. However, this argument may hold true under favorable, natural conditions, given that exotic species may have locally adapted, but not under conditions where multiple environmental stressors are present [27,28,37,39]. Indeed, there is evidence that exotic species perform better than indigenous species under stressful conditions, such as the urban environment [28]. Nonetheless, the difference in performance between exotic and indigenous species warrants

detailed assessment because the effect of gene and environment on species performance can be species-specific.

Located in north China, the Jing-Jin-Ji metropolitan region represents high urbanization. Consisting of Beijing, Tianjin, and Hebei province, the population in this region accounts for approximately 9% of the total in China. Vegetation in this area plays a pivotal role in regulating regional climate, mitigating the negative consequences of climate extremes, as well as offering recreational sites. Yet human activities, together with climate change-induced precipitation anomaly, are increasingly threatening the structure and function of vegetation, particularly tree species, as evidenced by the recorded drought-induced tree mortality in this area [40]. Therefore, knowledge about drought tolerance of urban forests can contribute to the sustainable development of this region.

Here, we report on the xylem embolism resistance in leaves for five angiosperm woody species common to urban forests in the Jing-Jin-Ji region. Tree mortality rate under water stress was also investigated to assess the functional significance of xylem embolism resistance in drought tolerance. In addition, leaf gas exchange traits were measured to test the potential tradeoff between efficiency and resistance. Moreover, morphological and leaf anatomical traits were also examined to search for easy proxies of physiological drought resistance. Importantly, the experimental plant materials included both introduced species and trees native to this region, thus allowing us to distinguish the adaptiveness between exotic and indigenous species. Specifically, we hypothesized that (1) species with more negative P_{50} would show less mortality rate under water deficit conditions; (2) there was a tradeoff between xylem embolism resistance and carbon acquisition, such that more embolism resistance species tended to have lower carbon assimilation; (3) leaf embolism resistance can be predicted from morphological or anatomical traits related to water balance. The findings will inform us how to establish and manage different urban tree species so that the functions of urban forests can be maintained in a sustainable way.

2. Materials and Methods

2.1. Plant Materials

This study was conducted at the Institute of Forestry and Pomology, Beijing Academy of Agriculture and Forestry Sciences, Beijing, China. This area has a semi-humid monsoon climate with dry-cold winter and hot-humid summer. The average annual precipitation and temperature are about 540 mm and 2–12 °C, respectively. Five deciduous, broad-leaf tree species commonly used for urban greening in the Jing-Jin-Ji metropolitan region were selected as the experimental materials: *Acer negundo* (abbreviation: Aneg), *Liriodendron* hybrids (Lhyb), *Acer truncatum* (Atru), *Koelreuteria paniculate* (Kpan), and *Cotinus coggygria* (Ccog). The first two species are exotic tree species in Beijing, while the latter three are indigenous species. In August 2020, more than 100 tree saplings of each species with a basal diameter of 2–3 cm and height of about 2 m were planted in PVC pots (39 cm diameter; 29 cm height), the mixed matrix (peat:perlite = 1:1) in which had a bulk density of 0.74 g cm^{-3} and a field water capacity (q_{fc}) of 0.35 cm^3 cm^{-3}. These potted trees were placed in a sunlit glass greenhouse of BAFPS and were manually irrigated twice to three times per week to ensure growth was not water limited.

Our experiment was formally initiated in June 2021. For each species, 72 potted trees with good growth status and no sign of pest attack or diseases infected were selected for the experiment. With the help of an automatic drip irrigation system, three water treatments were designed in our study for different purposes: (1) well-water treatment, in which the soil water content (q, cm^3 cm^{-3}) was kept between 85%–100% q_{fc}; (2) moderate water stress treatment, with q being kept at about 50% q_{fc}; and (3) severe water stress treatment, with q being around 20% q_{fc}. For every species, 24 potted trees were randomly selected from the aforementioned 72 trees and were assigned to each treatment. Due to limited space in the greenhouse, all trees in the well-water treatment were transferred outdoors throughout the experiment period for measuring physiological, morphological, and anatomical traits. Note that we only measured these traits in the well-water treatment to avoid any trait

change that might be induced by water stress [41]. The two water stress treatments were still conducted in the greenhouse and were only used to observe the final tree mortality rate three weeks after the experiment initiation.

2.2. Leaf Vulnerability Curve

The optical visualization method was applied to measure leaves' vulnerability curves (VC) from June to July 2021 [42]. As to each of the five species, three branches of about 100 cm in length were sampled from the sun-exposed middle canopy of three trees before dawn, when xylem tension reached the minimal value. The cut branches were immediately put into a bucket filled with distilled water. During branch sampling, a 15 cm long segment was cut from the branch base to diminish the influence of air entry into the functional vessels. Then, the branch samples were transported to the laboratory with the cut end maintained underwater. In the laboratory, the branches were covered with a black and opaque bag and placed in a dark environment to allow for complete rehydration. The well-rehydrated status of branches was confirmed when the water potential of three to four leaves randomly chosen from the branch reached above −0.5 MPa. After that, one mature leaf selected from the upper part of each branch was used for photographing using a custom-built clamp equipped with a micro camera (Raspberry Pi Camera Module v2, Raspberry Pi Foundation, Cambridge, UK), a bright LED light source, and a single-board computer (Raspberry Pi 3B+, Raspberry Pi Foundation). The photographing frequency was set to 10 min to capture the loss process of leaf vein hydraulic conductivity. Meanwhile, a psychrometer (PSY1, ICT International, Armidale, NSW, Australia) was applied to automatically measure the stem water potential (Ψ_{stem}) every 10 min, which was used as a surrogate for the leaf water potential (Ψ_{leaf}), considering the water potential difference between stem and leaves would be minimal for non-transpiring and dark-adapted branches.

Obtained leaf images were stacked, and the difference between two images taken consecutively, which was exhibited as black pixels, was revealed with the image difference function in Image J (National Institutes of Health, Bethesda, MD, USA). At any time point, the leaf embolism level, represented as the percentage loss of vein hydraulic conductivity (PLC), was estimated as the embolized pixel area divided by the total pixel area. The Ψ_{leaf} corresponding to each image was estimated by first fitting a linear relationship between Ψ_{stem} and time and then using the image timestamp as the independent variable. Finally, the VCs of leaves were developed by plotting the PLC of the leaf against Ψ_{leaf}.

2.3. Leaf Gas Exchange and Anatomical Traits

The photosynthetic light response curves of leaves were measured in situ using an infrared gas analyzer (Model 6800, Licor, Lincoln, NE, USA) equipped with an external CO_2 injector and a 2 × 3 cm cuvette with red-blue LED light sources. On sunny days from June to July 2021, three mature leaves selected from the fully sunlit upper canopy of three trees were used for measurements for each species. Before measurement, the photosynthetic machinery was activated by placing the leaf in the chamber supplied with 1200 μmol m^{-2} s^{-1} PFD (photon flux density) and 420 ppm CO_2 for at least 30 min until the reading of gas exchange variables was visually stable. Then, the net photosynthetic rate (A_{max}, μmol m^{-2} s^{-1}), transpiration rate (T_r, mmol m^{-2} s^{-1}), and stomatal conductance (g_s, mmol m^{-2} s^{-1}) were recorded at different PFD levels: 2000, 1800, 1500, 1200, 900, 600, 300, 200, 150, 100, 70, 30, and 0 μmol m^{-2} s^{-1}. The whole measurement was finished between 7:00–11:00 am. Afterward, we used the photosynthetic light-response model to fit the light-response characteristic parameters [43]. Subsequently, we estimated the maximum net photosynthetic rate (A_{max}) of each species.

For measuring leaf anatomical traits of each species, five healthy leaves were sampled from trees and then fixed in FAA (50% ethanol, 5% acetic acid, 10% formaldehyde). One leaf piece of about 5 mm × 5–10 mm was cut from each leaf at a position near the midvein to make the microscopic slide. In detail, we first embedded the leaf piece in paraffin and sliced a cross-section of about 10 μm thick by a rotary microtome (Leica RM2016, Leica,

Nusslock, Germany). Then, the leaf cross-section samples were washed using xylene, stained with Safranine and Fast Green, dehydrated with 85% ethanol, and finally mounted with neutral balsam. The microscopic slides were observed and photographed using an inverted fluorescence microscope (Leica DM4000B, Leica, Nusslock, Germany), and the CaseViewer software (Version 2.4.0119028, 3DHISTECH Inc., Budapest, Hungary) was used to analyze the images to measure various leaf anatomical traits, including leaf thickness, upper and lower epidermis thickness, palisade tissue thickness, sponge tissue thickness, and midvein thickness.

2.4. Leaf and Branch Morphological Traits

The traditional nail polish method was applied to measure stomatal density. First, the leaf surface needed to be cleaned, and the hair on the leaves of some tree species was scraped off with a blade or peeled off with sellotape. Then, the nail polish was evenly applied onto the upper middle part of the abaxial leaf surface, and when the nail polish was dry, it was pulled off the leaf surface by sellotape and mounted directly on the glass slide. We randomly selected six fields for each leaf print to observe the stomata distribution and measure its number at ×400 magnification using an optical microscope (Olympus BX43, Tokyo, Japan).

Six to ten leaves were sampled for each species in June–July 2021 for scanning to measure leaf surface area using the automatic image analysis software WinRHIZO (Regent Instruments Inc., Quebec, QC, Canada). After that, the leaves were dried to a constant weight at 70 °C in an oven. The specific leaf area (SLA, $cm^2\ g^{-1}$) was calculated as individual leaf surface area divided by individual leaf dry weight.

To investigate the variation pattern of leaf area with branch basal diameter, 20 branches attached with leaves were sampled for each species. After sampling, we measured the basal diameters of branches with the Vernier scale, while the total area of all leaves attached to a branch was measured using the automatic image analysis software WinRHIZO (Regent Instruments Inc., Quebec, QC, Canada). Then, the diameter and total leaf area of each branch were used to detect the relationship between them. In addition, we also calculated the ratio of branch basal diameter to leaf area distal to the branch, which can be considered as a surrogate for the Huber value to describe the water supply ability of the branch for leaf water demand.

We also sampled one-year-old branches from the upper canopy of each species to measure the wood density (WD, $g\ cm^{-3}$). A segment of 5 cm in length was excised from each branch sample, and its bark was removed immediately. Then, the fresh sapwood volume of each segment was determined with the water displacement method, and its dry weight was measured after drying the segment in an oven at 70 °C. The WD was estimated as the ratio of sapwood dry weight to its volume.

2.5. Data Analysis

We fitted the VCs of leaves with the sigmoidal model in the *fitplc* package in R to estimate the water potential thresholds that induced 12% (P_{12}, −MPa), 50% (P_{50}, −MPa), and 88% (P_{88}, −MPa) loss of leaf hydraulic conductivity. To obtain information on the embolism development speed with decreasing Ψ_{leaf}, we calculated the leaf hydraulic safety margin (HSM, −MPa) as P_{50}–P_{12} [28]. The HSM, together with the three metrics obtained from the VCs, can help to evaluate the different species' drought tolerance comprehensively.

One-way analysis of variance (ANOVA) was conducted to analyze the difference among tree species in plant physiological (HSM, P_{12}, P_{50}, P_{88}, A_{max}; T_r and g_s at PPFD level of 1500 $\mu mol\ m^{-2}\ s^{-1}$), morphological (SLA, WD, SD), and anatomical (thickness of leaf, midvein, upper lower epidermis, sponge tissue, and palisade tissue) traits. When ANOVA detected a significant overall species effect ($p < 0.05$), the species means were compared with the Tukey HSD test. Before these analyses, the Kolmogorov–Smirnov test and the Levene test were first used to verify whether the data of each variable met the assumptions

of normality and homogeneity of variances, and the data were log-transformed when the assumptions were not met.

Linear regressions were applied to investigate the relationships between physiological, morphological, anatomical, and growth traits. The power function ($y = ax^b$) was used to fit the nonlinear relationship between leaf area and branch basal diameter, and then an *F*-test was applied to detect whether there were significant differences in the parameters of the fitted curves between the indigenous and exotic species.

The ANOVA and regression analyses in our study were conducted using OriginPro 2022 (OriginLab Corporation, Northampton, MA, USA).

3. Results

3.1. Leaf Embolism Resistance

There was a significant difference in the leaf embolism resistance, characterized by P_{50}, among different tree species ($p < 0.05$) (Figures 1 and 2). Ccog exhibited the highest resistance to leaf embolism (i.e., having the most negative P_{50}), which was followed by Atru, Kpan, Lhyb, and Aneg in sequence. The other two metrics describing leaf embolism resistance, i.e., P_{12} and P_{88}, also varied markedly across tree species ($p < 0.05$), and the order in them among species was the same as that in P_{50} (Figure 2). The HSM of various species was significantly different from each other ($p < 0.05$), with Atru and Aneg having the widest and narrowest HSM, respectively (Figure 2). Unexpectedly, no correlation was detected between HSM and P_{50} for the five investigated species ($p = 0.221$). In addition, the indigenous species showed obviously more negative average P_{12}, P_{50}, and P_{88} and had wider average HSM (indigenous: −1.31 MPa vs. exotic: −0.55 MPa) than the exotic species (Figure 2).

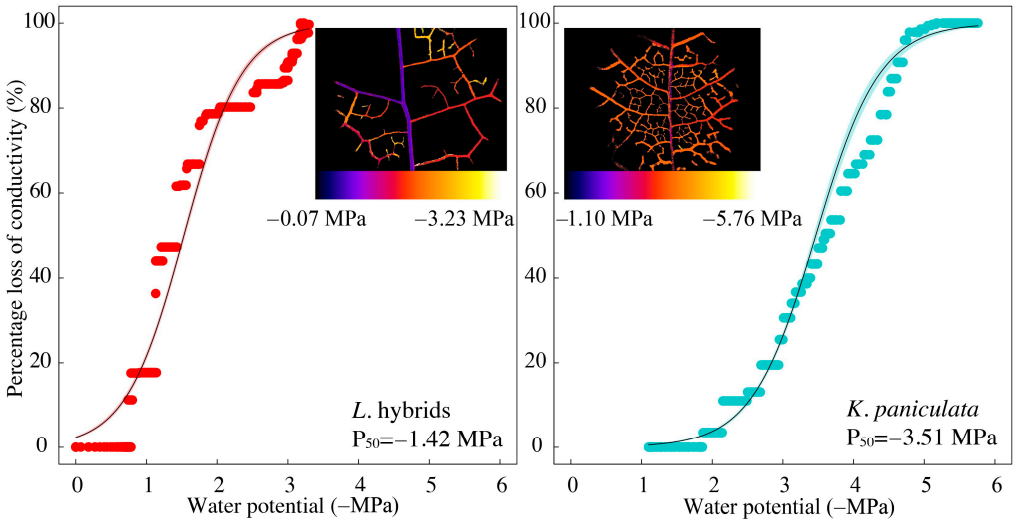


Figure 1. The vulnerability curves, measured with the optical visualization technique, of representative exotic (*Liriodendron* hybrids) and indigenous (*Koelreuteria paniculate*) tree species. The inset figures show the spatiotemporal development of embolism within the leaf vein network during dehydration. Water potential during leaf dehydration is indicated by color, with cool and warm color representing less negative and more negative water potentials, respectively.

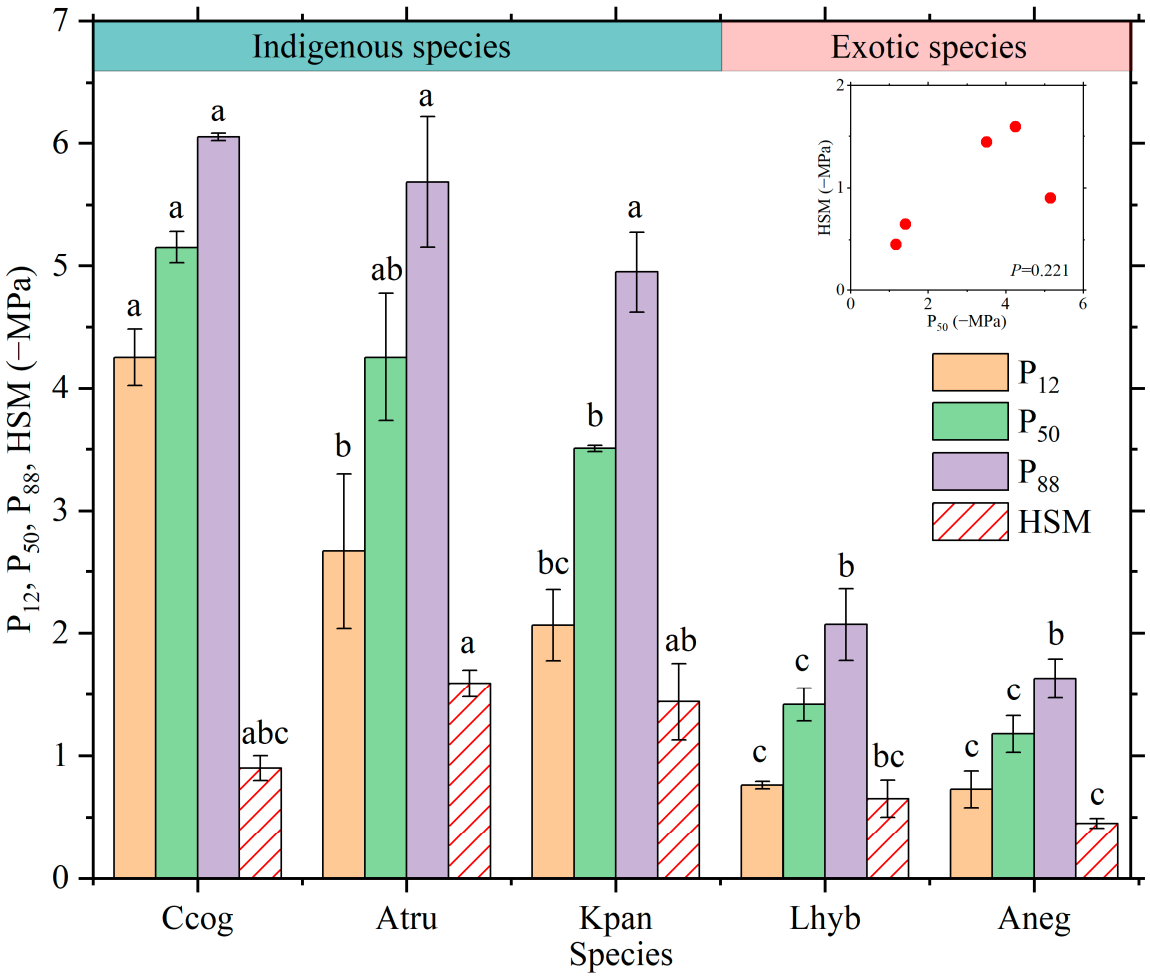


Figure 2. Variations of different metrics describing the leaf embolism resistance among tree species. The inset figure shows the relationship between P_{50} and the hydraulic safety margin (HSM). P_{12}, P_{50}, and P_{88} are the water potential inducing 12%, 50%, and 88% loss of leaf hydraulic conductivity. The error bar represents standard error. Different lowercase letters on the columns belonging to the same metric indicate significant differences across species at $p \leq 0.05$, according to the Tukey HSD test.

3.2. Variation of Leaf Area with Branch Basal Diameter

For all species, there was a good nonlinear relationship between leaf area and branch basal diameter ($p < 0.001$) (Figure 3). However, the increasing rate of leaf area with branch diameter changed markedly across species. This indicates that there is a difference in the sapwood area for supporting the same area of leaves among species, and this difference will increase for larger branches. Furthermore, the variation pattern of leaf area with branch diameter significantly differed between the exotic and indigenous species (the parameter a of the fitted power function was different at $p = 0.049$), with the indigenous species having more sapwood to transfer water to the same leaf area, or in other words, the indigenous species possessing more leaves with the same sapwood area.

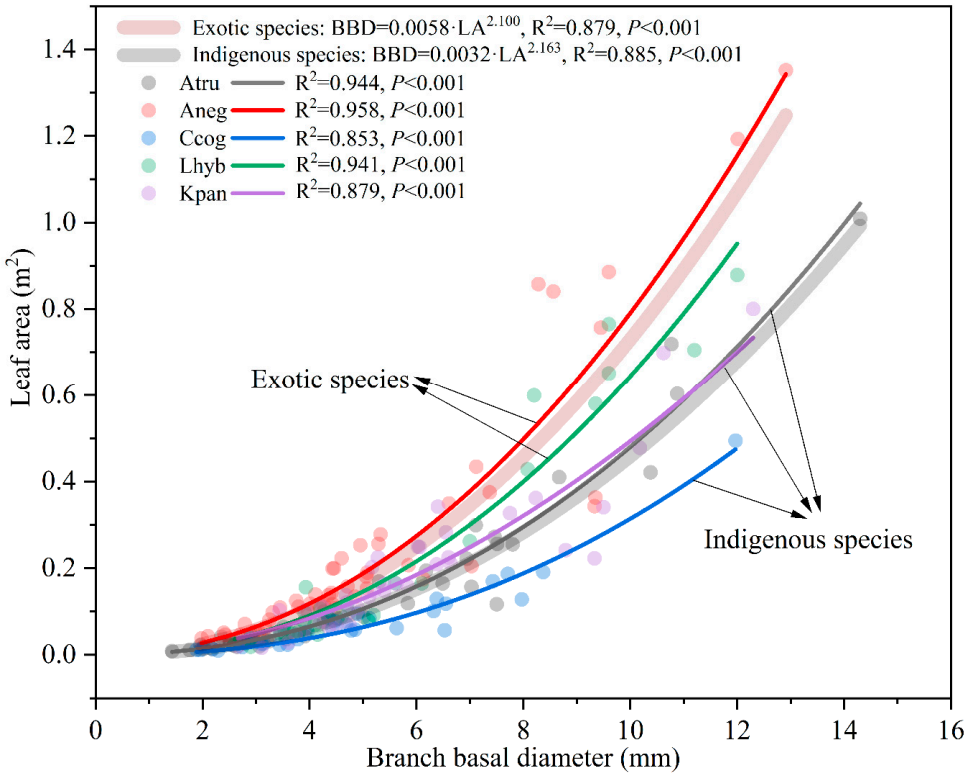


Figure 3. Variations of leaf area with branch basal diameter for different tree species. Curves of different colors are fitted curves for different tree species, and the R^2 and *p* values of these nonlinear regressions are also shown in the figure.

3.3. Relationship between Tree Mortality Rate and Plant Hydraulics

Under both moderate and severe water stress conditions, the species with more negative P_{50} tended to have a lower final mortality rate (Figure 4). Nonetheless, no obvious influence of HSM on tree mortality rate was observed ($p > 0.05$).

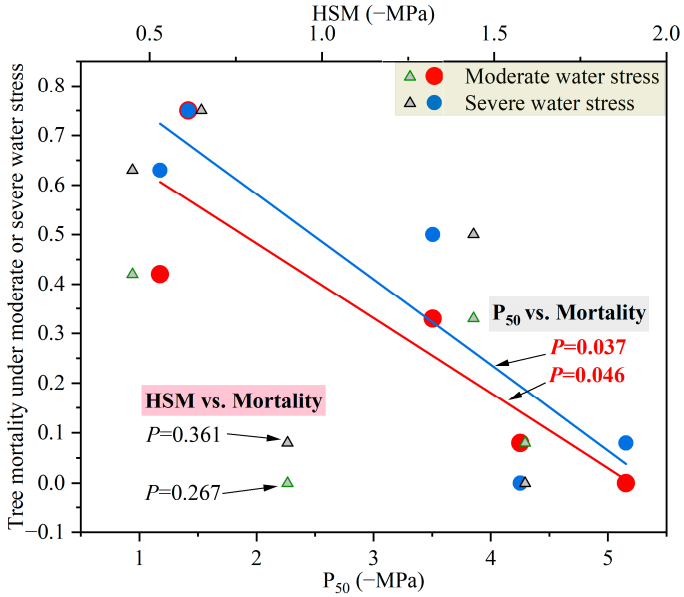


Figure 4. The relationships between tree mortality rate and water potential at 50% loss of leaf hydraulic conductivity (P_{50}) and hydraulic safety margin (HSM) under different water stress degrees.

3.4. Correlations among Physiological, Morphological, and Anatomical Traits

Significant differences among species were found for all measured plant physiological (A_{max}, T_r, g_s), morphological (SLA, WD, SD), and anatomical (thickness of midvein, leaf, upper epidermis, lower epidermis, sponge tissue, and palisade tissue) traits ($p < 0.01$) (Table 1). The A_{max} showed significantly positive and negative linear relationships with P_{50} and SLA, respectively, but no significant correlations were detected between A_{max} and HSM and branch diameter/leaf area (Figure 5).

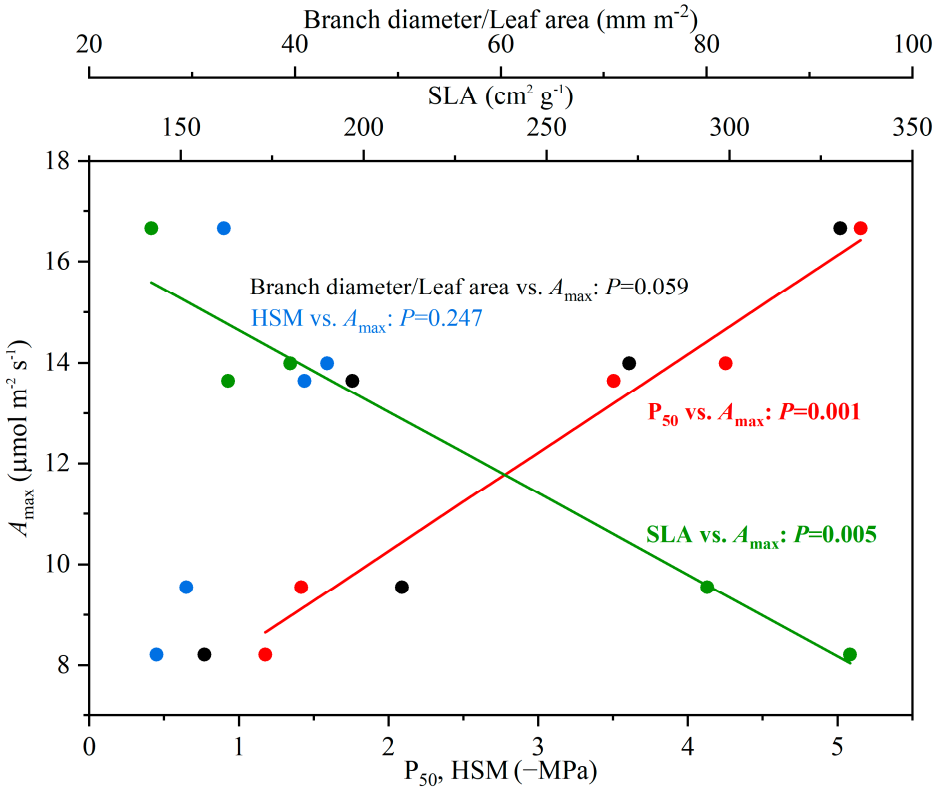


Figure 5. The correlations between maximum photosynthetic rate (A_{max}) and water potential at 50% loss of leaf hydraulic conductivity (P_{50}), hydraulic safety margin (HSM), specific leaf area (SLA), as well as branch diameter/leaf area.

The variation in leaf embolism resistance among species was not related to most morphological and anatomical traits ($p > 0.05$), but the species with smaller SLA was more resistant to drought-induced leaf embolism (i.e., having more negative P_{50}) (Figures 6 and 7). Similarly, no significant correlation existed between HSM and most morphological and anatomical traits ($p > 0.05$) (Figures 6 and 7). However, it was found that species with higher branch wood density and thicker leaf upper epidermis possessed a wider HSM.

Table 1. The physiological, morphological, and anatomical traits of five tree species. A_{max}, maximum photosynthetic rate; Tr, transpiration rate at PPFD level of 1500 μmol m^{-2} s^{-1}; g_s, stomatal conductance at PPFD level of 1500 μmol m^{-2} s^{-1}; SLA, specific leaf area; WD, wood density; SD, stomata density. Different lowercase letters within the same column indicate significant differences among species at $p \leq 0.05$, according to the Tukey HSD test. The number in the bracket indicates the standard error.

Species	A_{max} (μmol m^{-2} s^{-1})	T_r (mmol m^{-2} s^{-1})	g_s (mmol m^{-2} s^{-1})	SLA (cm^2 g^{-1})	WD (g cm^{-3})	SD (number m^{-2})	Midvein Thickness (μm)	Leaf Thickness (μm)	Upper Epidermis Thickness (μm)	Lower Epidermis Thickness (μm)	Sponge Tissue Thickness (μm)	Palisade Tissue Thickness (μm)
Lhyb	9.55 (0.12) c	1.83 (0.05) ab	0.08 (0.00) c	294 (11) b	0.366 (0.01) d	304 (7) c	689 (29) b	187 (3) a	16 (1) b	14 (1) a	81 (2) a	77 (1) a
Aneg	8.21 (0.74) c	1.50 (0.18) b	0.11 (0.01) bc	333 (8) a	0.278 (0.02) e	821 (22) a	516 (1) c	106 (2) d	13 (0) b	9 (0) b	55 (1) c	30 (1) c
Kpan	13.64 (0.18) b	4.87 (1.15) a	0.13 (0.00) abc	163 (8) cd	0.602 (0.01) a	744 (18) a	935 (4) a	162 (2) b	21 (1) a	10 (0) b	75 (1) b	57 (2) b
Atru	13.99 (0.02) b	4.52 (0.93) ab	0.18 (0.03) ab	180 (7) c	0.524 (0.01) b	570 (22) b	345 (17) d	129 (3) c	24 (2) a	11 (1) b	60 (1) c	35 (3) c
Ccog	16.66 (0.74) a	2.68 (0.23) ab	0.20 (0.02) a	142 (1) d	0.449 (0.02) c	616 (51) b	707 (4) b	127 (2) c	16 (1) b	10 (1) b	7 (1) b	29 (2) c

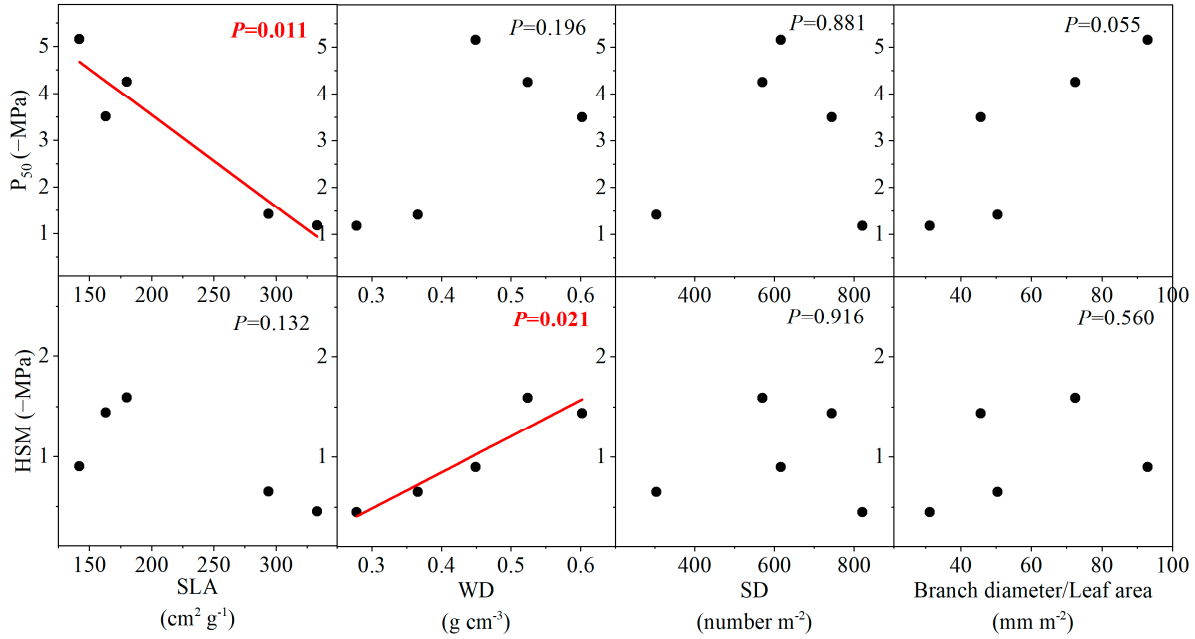


Figure 6. The relationships between water potential at 50% loss of leaf hydraulic conductivity (P_{50}), hydraulic safety margin (HSM), and different morphological traits. SLA, WD, and SD are specific leaf area, wood density, and stomata density, respectively.

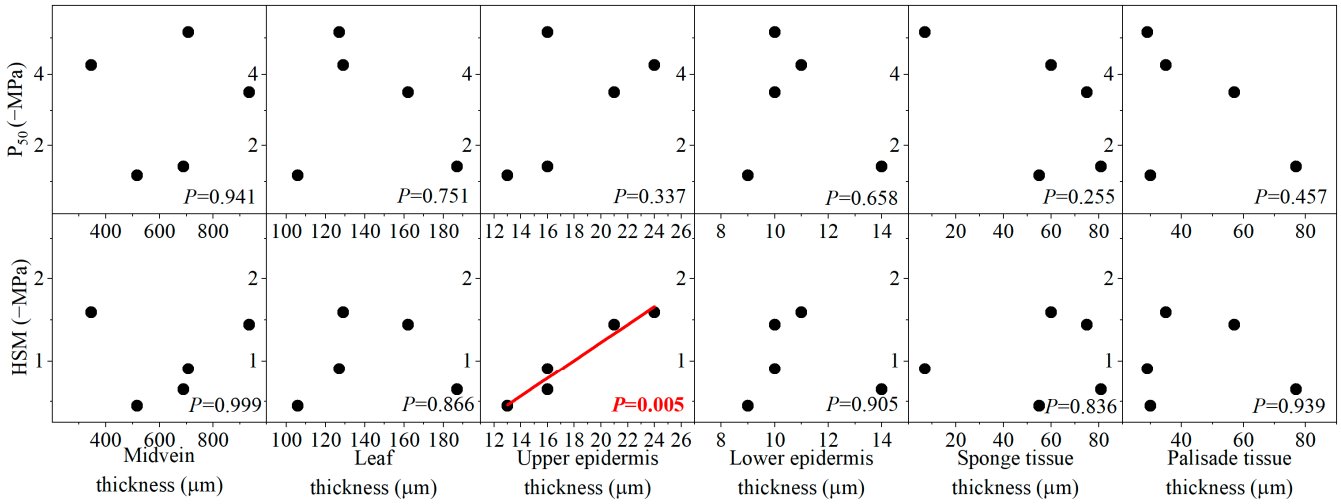


Figure 7. The relationships between water potential at 50% loss of leaf hydraulic conductivity (P_{50}), hydraulic safety margin (HSM), and different leaf anatomical traits.

4. Discussion

4.1. Indigenous Species Are More Drought-Resistant Than Exotic Species

Xylem embolism resistance, quantified by water potential triggering 50% loss of xylem hydraulic conductance (P_{50}), is often measured for stems, while P_{50} of leaves is currently represented by relatively few species, especially for P_{50} values measured exclusively for the xylem water transport pathway. Of the five species examined in the current study, leaf P_{50} values of Ccog and Atru were similar to those reported by [28] using the same technique, while P_{50} of Lhyb was comparable to the value of *Liriodendron tulipifera*, one of the parent species for this hybrid, measured with X-ray microcomputed tomography method [44]. Overall, leaf P_{50} showed considerable variation across the five species (Figure 2), indicating significant discrepancy in drought resistance for current tree species within the urban forest of this region. Of note, plant materials used in [28] were collected from field-grown, mature

trees, while leaves measured in the current study were obtained from pot-grown sapling plants. The similarities in P_{50} value for trees with contrasting age and growth conditions suggested that xylem embolism resistance was largely canalized in these species and thus may not alter under varying environmental conditions [45], as has been reported in other species [23]. This clearly bolsters the usefulness of this trait in guiding species screening, given that plastic P_{50} would add complexity in forecasting tree performance when stress such as water deficit occurs. Importantly, we found that indigenous tree species showed more negative P_{50} compared with exotic species (Figure 2), indicating that local species were more resistant to drought and thus may outperform exotic tree species under drought.

On the other hand, we found that the two exotic species exhibited a higher leaf area to basal diameter ratio than the indigenous species (Figure 3), suggesting that these species can support more leaf area for a given occupied area. Given that this metric primarily reflects the supply–demand relationship for water use, variation in this ratio can be attributed to multiple aspects related to water balance [41,46]. Firstly, the ratio can increase as water demand decreases at the leaf scale. In support, we found that the two exotic species showed obviously lower rates of g_s and T_r, probably because of decreased stomata aperture, as stomatal density did not differ systematically between exotic and indigenous species (Table 1). Secondly, the ratio can also increase due to a higher water supply, which is mediated by the hydraulic conductivity of the trunk. Unfortunately, the sap flow rate was not measured in the current study. Nonetheless, we found that exotic tree species generally exhibited low WD (Table 1), which is often found to be inversely associated with the water transport capacity of plants [23,47]. Therefore, higher hydraulic conductivity in exotic species may also have contributed to the increased leaf area to basal diameter ratio, although the possibility needs to be verified by further experimental evidence.

4.2. Xylem Embolism Predicts Tree Mortality Rate under Drought Stress

We found that leaf P_{50} was a robust predictor for tree mortality rate during drought stress, regardless of the intensity of water deficit (Figure 4), thus underscoring the functional significance of embolism resistance in defining vegetation dynamics under drought [11,12,21]. It has been hypothesized that drought-induced tree mortality is primarily attributed to hydraulic failure, i.e., the loss of xylem hydraulic conductivity due to embolism, which has later been validated by a number of experimental studies using diverse species, with gymnosperm species typically dying when xylem embolism level exceeds 50% [19], while mortality of angiosperm species requires >88% or complete loss of xylem hydraulic conductivity [20,48]. Noticeably, many of these studies focused on the mortality thresholds at the individual level, while the point of no return for hydraulic failure at the population level was largely understudied. Nonetheless, it appeared that tree demography under water deficit conditions can also be inferred from individual-level traits. For example, Zhu et al. (2018) showed that the survival ratio of tree species was related to species-specific P_{50}. Likewise, mortality for most *Pinus taeda* individuals occurred when ca. 80% xylem hydraulic conductivity was lost [49]. These results, together with the observation in the current study, clearly reinforce the universality of embolism resistance in dictating tree dynamics under drought at various ecological scales.

4.3. Increased Embolism Resistance Does Not Compromise Carbon Assimilation

Our results did not support the proposed tradeoff between carbon acquisition and xylem embolism resistance (Figure 5). On the contrary, a positive correlation was found between P_{50} and A_{max}, suggesting that species characterized by strong drought resistance were also efficient in assimilating carbon at given leaf area. Such finding contrasts the proposed interspecific traits relationship according to the "fast-slow" spectrum, which states a tradeoff between traits conferring resource acquisition and stress tolerance [50], as well as studies showing a negative correlation between P_{50} and A_{max} [35,51]. However, the relationship between carbon assimilation and drought resistance appears highly variable across studies. For instance, a positive relationship between A_{max} and P_{50}, as we identified

in the current study, was reported across a wide range of tree species originating from sites characterized by contrasting climates [23], while Han et al. (2022) found no correlation between these two traits. It is possible that the interspecific relationship between carbon assimilation and embolism resistance can be influenced by the light environment, such that sun and shade leaves would differently associate with embolism resistance because of contrasting gas exchange efficiency, photosynthetic biochemistry, or water status. However, gas exchange traits were consistently measured from leaves of the upper canopy, where the light environment was comparable across individuals and species, thus it was unlikely to confound the traits' correlation. Evidently, the relationship between xylem embolism resistance and carbon assimilation can vary across different sets of species, thus necessitating the need for thorough assessment when balancing the benefit between stress tolerance and productivity for candidate species.

4.4. Morphological Traits Are Better Surrogates of Physiological Drought Tolerance

The negative correlation between P_{50} and SLA indicated that leaf embolism resistance can be predicted from leaf morphology (Figure 6). Such correlation was somewhat unexpected given that the relationship between these two traits is only theoretically possible. It has been proposed that a tradeoff could exist between traits conferring stress resistance and quantifying the efficiency of resource acquisition, such as P_{50} and SLA, respectively [50]. However, it is worth noting that the correlation between these two traits emerges as a result of co-selection rather than a mechanistic linkage, given that P_{50} and SLA differ largely in regard to structural basis. Yet, such a tradeoff has only been supported by very limited empirical evidence. However, it has been shown that the likelihood of drought-induced tree mortality can be predicted by SLA, such that species with high SLA showed an increased possibility of dieback under drought at the global scale [52]. Considering the mechanistic linkage between hydraulic failure and tree mortality under drought, it could be speculated that SLA should relate to P_{50}. Presumably, the correlation between SLA and P_{50} can be highly specific. For example, for six species distributed along a water availability gradient, SLA was found to correlate with P_{50} in two species [25].

On the other hand, we found that HSM can be predicted by both WD and the thickness of the upper epidermis (Figures 6 and 7). In the present study, we defined HSM as the difference between P_{50} and P_{12}. Thus, this metric can be taken as the proxy of the slope for the vulnerability curve, which reflects the speed of embolism spread within the vascular network during dehydration [47]. The positive correlation between HSM and WD was consistent with the findings in some studies, showing that species with dense wood tend to show a slow increase in xylem embolism under increasing xylem tension [53]. However, it is worth noting that such a relationship may not reflect a mechanistic linkage, given that WD is a highly integrated trait incorporating many features independent of species susceptibility to embolism [32,54]. In contrast, the thickness of the leaf upper epidermis can exert strong control over water loss after the complete close of stomata and, therefore, can regulate the spread of xylem embolism by governing xylem tension, consequently leading to the correlation with HSM [55].

5. Conclusions

The ecosystem service of urban forests is increasingly compromised by drought stress triggered by both climate change and human activity. Conservation and establishment of tree species within urban forests require knowledge regarding their drought resistance as well as potential tradeoffs, which can provide valuable information guiding species screening and forest management after planting. By investigating key physiological traits defining species drought resistance for five urban forest species common to regions characterized by high levels of urbanization in north China, we showed that considerable variation existed in leaf embolism resistance across species, with indigenous species being more tolerant to drought-induced embolism compared with exotic species, as evidenced by more negative P_{50} and wider HSM. Meanwhile, due to the lack of tradeoff between

embolism resistance and leaf photosynthesis, indigenous species were also advantageous in carbon acquisition. Therefore, these species can be preferentially considered for sites where soil water availability is limited and atmospheric water demand is high, such as streets or sites where irrigation measure is not convenient to be applied or with a high portion of impervious surface. Although less capable of assimilating carbon and resisting drought, exotic species can develop more leaf area within a limited area due to the high leaf area to basal diameter ratio and help to increase the diversity of tree species and the scenic beauty of urban forests. Hence, these exotic species may require periodic human intervention such as irrigation or trimming to minimize the risk of exposure to drought stress and can be suitable for sites with better moisture conditions and where shading is much needed, such as parks. Moreover, the correlations between embolism resistance and morphological or anatomical traits indicate that physiological drought tolerance can be predicted from easily measured proxies. If widespread, traits such as SLA or WD can be utilized as a quick screening tool for species selection. The current work focused only on key hydraulic traits associated with drought tolerance, with limited species. Further study could extend measured traits to those exerting control over water transport efficiency and water loss, as well as different growth forms including shrubs and herbs, thus enabling deeper and more comprehensive insights into the water use strategy of urban forests. In addition, additional studies that investigate the water status at both spatial and temporal scales are solicited, which would help to precisely assess the risk of exposure to drought-induced canopy dieback or tree mortality. Overall, our results add to the current knowledge regarding species drought tolerance in urban ecosystems and can offer guidance for establishing and managing urban forests in this region.

Author Contributions: Y.W. and G.L. designed the research. Y.W., T.L. and L.G. performed the research. Y.W. and B.X. analyzed data. Y.W., B.X. and G.L. wrote the paper. T.L. and L.G. revised the manuscript. All authors have read and agreed to the published version of the manuscript.

Funding: This work was supported by the fund of Beijing Academy of Agriculture and Forestry Sciences Scientific and Technological Innovation Ability construction (KJCX20230209), and the National Forestry and Grassland Germplasm Resources bank (2005DKA21003).

Data Availability Statement: The data presented in this study are available on request from the corresponding author.

Conflicts of Interest: The authors declare no conflict of interest.

References

1. Dai, A. Increasing drought under global warming in observations and models. *Nat. Clim. Chang.* **2013**, *3*, 52–58. [CrossRef]
2. Loukas, A.; Vasiliades, L.; Tzabiras, J. Climate change effects on drought severity. *Adv. Geosci.* **2008**, *17*, 23–29. [CrossRef]
3. Esperon-Rodriguez, M.; Tjoelker, M.G.; Lenoir, J.; Baumgartner, J.B.; Beaumont, L.J.; Nipperess, D.A.; Power, S.A.; Richard, B.; Rymer, P.D.; Gallagher, R.V. Climate change increases global risk to urban forests. *Nat. Clim. Chang.* **2022**, *12*, 950–955. [CrossRef]
4. Zhang, X.; Chen, N.; Sheng, H.; Ip, C.; Yang, L.; Chen, Y.; Sang, Z.; Tadesse, T.; Lim, T.P.Y.; Rajabifard, A. Urban drought challenge to 2030 sustainable development goals. *Sci. Total Environ.* **2019**, *693*, 133536. [CrossRef] [PubMed]
5. Endreny, T.; Sica, F.; Nowak, D. Tree cover is unevenly distributed across cities globally, with lowest levels near highway pollution sources. *Front. Sustain. Cities* **2020**, *2*, 16. [CrossRef]
6. Brandt, L.; Lewis, A.D.; Fahey, R.; Scott, L.; Darling, L.; Swanston, C. A framework for adapting urban forests to climate change. *Environ. Sci. Policy* **2016**, *66*, 393–402. [CrossRef]
7. Grimm, N.B.; Faeth, S.H.; Golubiewski, N.E.; Redman, C.L.; Wu, J.; Bai, X.; Briggs, J.M. Global change and the ecology of cities. *Science* **2008**, *319*, 756–760. [CrossRef]
8. Huang, K. Urban forests facing climate risks. *Nat. Clim. Chang.* **2022**, *12*, 893–894. [CrossRef]
9. Ordóñez, C.; Duinker, P.N. Assessing the vulnerability of urban forests to climate change. *Environ. Rev.* **2014**, *22*, 311–321. [CrossRef]
10. Sjöman, H.; Hirons, A.D.; Bassuk, N.L. Urban forest resilience through tree selection—Variation in drought tolerance in Acer. *Urban For. Urban Green.* **2015**, *14*, 858–865. [CrossRef]
11. Brodribb, T.J.; Powers, J.; Cochard, H.; Choat, B. Hanging by a thread? Forests and drought. *Science* **2020**, *368*, 261–266. [CrossRef] [PubMed]

12. Choat, B.; Brodribb, T.J.; Brodersen, C.R.; Duursma, R.A.; López, R.; Medlyn, B.E. Triggers of tree mortality under drought. *Nature* **2018**, *558*, 531–539. [CrossRef] [PubMed]
13. Angeles, G.; Bond, B.; Boyer, J.S.; Brodribb, T.; Brooks, J.R.; Burns, M.J.; Cavender-Bares, J.; Clearwater, M.; Cochard, H.; Comstock, J. The cohesion-tension theory. *New Phytol.* **2004**, *163*, 451–452.
14. Dixon, H.H.; Joly, J. On the ascent of sap. *Proc. R. Soc. Lond.* **1894**, *57*, 3–5. [CrossRef]
15. Zimmermann, U.; Schneider, H.; Wegner, L.H.; Haase, A. Water ascent in tall trees: Does evolution of land plants rely on a highly metastable state? *New Phytol.* **2004**, *162*, 575–615. [CrossRef] [PubMed]
16. Cochard, H.; Cruiziat, P.; Tyree, M.T. Use of positive pressures to establish vulnerability curves: Further support for the air-seeding hypothesis and implications for pressure-volume analysis. *Plant Physiol.* **1992**, *100*, 205–209. [CrossRef]
17. Mayr, S.; Kartusch, B.; Kikuta, S. Evidence for air-seeding: Watching the formation of embolism in conifer xylem. *J. Plant Hydraul.* **2014**, *1*, e004. [CrossRef]
18. Sperry, J.S.; Tyree, M.T. Mechanism of water stress-induced xylem embolism. *Plant Physiol.* **1988**, *88*, 581–587. [CrossRef]
19. Brodribb, T.J.; Cochard, H. Hydraulic failure defines the recovery and point of death in water-stressed conifers. *Plant Physiol.* **2009**, *149*, 575–584. [CrossRef]
20. Urli, M.; Porté, A.J.; Cochard, H.; Guengant, Y.; Burlett, R.; Delzon, S. Xylem embolism threshold for catastrophic hydraulic failure in angiosperm trees. *Tree Physiol.* **2013**, *33*, 672–683. [CrossRef]
21. Lens, F.; Tixier, A.; Cochard, H.; Sperry, J.S.; Jansen, S.; Herbette, S. Embolism resistance as a key mechanism to understand adaptive plant strategies. *Curr. Opin. Plant Biol.* **2013**, *16*, 287–292. [CrossRef]
22. Trueba, S.; Pouteau, R.; Lens, F.; Feild, T.S.; Isnard, S.; Olson, M.E.; Delzon, S. Vulnerability to xylem embolism as a major correlate of the environmental distribution of rain forest species on a tropical island. *Plant Cell Environ.* **2017**, *40*, 277–289. [CrossRef]
23. Li, X.; Blackman, C.J.; Choat, B.; Duursma, R.A.; Rymer, P.D.; Medlyn, B.E.; Tissue, D.T. Tree hydraulic traits are coordinated and strongly linked to climate-of-origin across a rainfall gradient. *Plant Cell Environ.* **2018**, *41*, 646–660. [CrossRef]
24. Peters, J.M.; López, R.; Nolf, M.; Hutley, L.B.; Wardlaw, T.; Cernusak, L.A.; Choat, B. Living on the edge: A continental-scale assessment of forest vulnerability to drought. *Glob. Chang. Biol.* **2021**, *27*, 3620–3641. [CrossRef]
25. Rosas, T.; Mencuccini, M.; Barba, J.; Cochard, H.; Saura-Mas, S.; Martínez-Vilalta, J. Adjustments and coordination of hydraulic, leaf and stem traits along a water availability gradient. *New Phytol.* **2019**, *223*, 632–646. [CrossRef] [PubMed]
26. Choat, B.; Jansen, S.; Brodribb, T.J.; Cochard, H.; Delzon, S.; Bhaskar, R.; Bucci, S.J.; Feild, T.S.; Gleason, S.M.; Hacke, U.G. Global convergence in the vulnerability of forests to drought. *Nature* **2012**, *491*, 752–755. [CrossRef] [PubMed]
27. Esperon-Rodriguez, M.; Rymer, P.D.; Power, S.A.; Challis, A.; Marchin, R.M.; Tjoelker, M.G. Functional adaptations and trait plasticity of urban trees along a climatic gradient. *Urban For. Urban Green.* **2020**, *54*, 126771. [CrossRef]
28. Han, H.; Xi, B.; Wang, Y.; Feng, J.; Li, X.; Tissue, D.T. Lack of phenotypic plasticity in leaf hydraulics for 10 woody species common to urban forests of North China. *Tree Physiol.* **2022**, *42*, 1203–1215. [CrossRef]
29. Savi, T.; Bertuzzi, S.; Branca, S.; Tretiach, M.; Nardini, A. Drought-induced xylem cavitation and hydraulic deterioration: Risk factors for urban trees under climate change? *New Phytol.* **2015**, *205*, 1106–1116. [CrossRef]
30. Blackman, C.J.; Li, X.; Choat, B.; Rymer, P.D.; De Kauwe, M.G.; Duursma, R.A.; Tissue, D.T.; Medlyn, B.E. Desiccation time during drought is highly predictable across species of Eucalyptus from contrasting climates. *New Phytol.* **2019**, *224*, 632–643. [CrossRef] [PubMed]
31. Bittencourt, P.R.; Pereira, L.; Oliveira, R.S. On xylem hydraulic efficiencies, wood space-use and the safety–efficiency tradeoff. *New Phytol.* **2016**, *211*, 1152–1155. [CrossRef] [PubMed]
32. Gleason, S.M.; Westoby, M.; Jansen, S.; Choat, B.; Hacke, U.G.; Pratt, R.B.; Bhaskar, R.; Brodribb, T.J.; Bucci, S.J.; Cao, K.F. Weak tradeoff between xylem safety and xylem-specific hydraulic efficiency across the world's woody plant species. *New Phytol.* **2016**, *209*, 123–136. [CrossRef] [PubMed]
33. Brodribb, T.; Holbrook, N.M.; Gutierrez, M. Hydraulic and photosynthetic co-ordination in seasonally dry tropical forest trees. *Plant Cell Environ.* **2002**, *25*, 1435–1444. [CrossRef]
34. Santiago, L.S.; Goldstein, G.; Meinzer, F.C.; Fisher, J.B.; Machado, K.; Woodruff, D.; Jones, T. Leaf photosynthetic traits scale with hydraulic conductivity and wood density in Panamanian forest canopy trees. *Oecologia* **2004**, *140*, 543–550. [CrossRef]
35. Maherali, H.; Moura, C.F.; Caldeira, M.C.; Willson, C.J.; Jackson, R.B. Functional coordination between leaf gas exchange and vulnerability to xylem cavitation in temperate forest trees. *Plant Cell Environ.* **2006**, *29*, 571–583. [CrossRef] [PubMed]
36. van der Sande, M.T.; Poorter, L.; Schnitzer, S.A.; Engelbrecht, B.M.; Markesteijn, L. The hydraulic efficiency–safety trade-off differs between lianas and trees. *Ecology* **2019**, *100*, e02666. [CrossRef]
37. Sjöman, H.; Morgenroth, J.; Sjöman, J.D.; Sæbø, A.; Kowarik, I. Diversification of the urban forest—Can we afford to exclude exotic tree species? *Urban For. Urban Green.* **2016**, *18*, 237–241. [CrossRef]
38. Sagoff, M. Do non-native species threaten the natural environment? *J. Agric. Environ. Ethics* **2005**, *18*, 215–236. [CrossRef]
39. Roloff, A.; Korn, S.; Gillner, S. The Climate-Species-Matrix to select tree species for urban habitats considering climate change. *Urban For. Urban Green.* **2009**, *8*, 295–308. [CrossRef]
40. Zhang, X.; Lei, Y.; Pang, Y.; Liu, X.; Wang, J. Tree mortality in response to climate change induced drought across Beijing, China. *Clim. Chang.* **2014**, *124*, 179–190. [CrossRef]
41. Guo, Y.; Ma, Y.; Ding, C.; Di, N.; Liu, Y.; Tan, J.; Zhang, S.; Yu, W.; Gao, G.; Duan, J. Plant hydraulics provide guidance for irrigation management in mature polar plantation. *Agric. Water Manag.* **2023**, *275*, 108029. [CrossRef]

42. Brodribb, T.J.; Skelton, R.P.; McAdam, S.A.; Bienaimé, D.; Lucani, C.J.; Marmottant, P. Visual quantification of embolism reveals leaf vulnerability to hydraulic failure. *New Phytol.* **2016**, *209*, 1403–1409. [CrossRef]
43. Ye, Z.-P.; Yu, Q. Comparison of new and several classical models of photosynthesis in response to irradiance. *Chin. J. Plant Ecol.* **2008**, *32*, 1356.
44. Klepsch, M.; Zhang, Y.; Kotowska, M.M.; Lamarque, L.J.; Nolf, M.; Schuldt, B.; Torres-Ruiz, J.M.; Qin, D.-W.; Choat, B.; Delzon, S. Is xylem of angiosperm leaves less resistant to embolism than branches? Insights from microCT, hydraulics, and anatomy. *J. Exp. Bot.* **2018**, *69*, 5611–5623. [CrossRef]
45. Lamy, J.B.; Delzon, S.; Bouche, P.S.; Alia, R.; Vendramin, G.G.; Cochard, H.; Plomion, C. Limited genetic variability and phenotypic plasticity detected for cavitation resistance in a M editerranean pine. *New Phytol.* **2014**, *201*, 874–886. [CrossRef]
46. Zhu, L.-W.; Zhao, P. Climate-driven sapwood-specific hydraulic conductivity and the Huber value but not leaf-specific hydraulic conductivity on a global scale. *Sci. Total Environ.* **2023**, *857*, 159334. [CrossRef]
47. Meinzer, F.C.; Johnson, D.M.; Lachenbruch, B.; McCulloh, K.A.; Woodruff, D.R. Xylem hydraulic safety margins in woody plants: Coordination of stomatal control of xylem tension with hydraulic capacitance. *Funct. Ecol.* **2009**, *23*, 922–930. [CrossRef]
48. Blackman, C.J.; Brodribb, T.J.; Jordan, G.J. Leaf hydraulics and drought stress: Response, recovery and survivorship in four woody temperate plant species. *Plant Cell Environ.* **2009**, *32*, 1584–1595. [CrossRef] [PubMed]
49. Hammond, W.M.; Yu, K.; Wilson, L.A.; Will, R.E.; Anderegg, W.R.; Adams, H.D. Dead or dying? Quantifying the point of no return from hydraulic failure in drought-induced tree mortality. *New Phytol.* **2019**, *223*, 1834–1843. [CrossRef] [PubMed]
50. Reich, P.B. The world-wide 'fast–slow'plant economics spectrum: A traits manifesto. *J. Ecol.* **2014**, *102*, 275–301. [CrossRef]
51. Zhu, S.-D.; Chen, Y.-J.; Ye, Q.; He, P.-C.; Liu, H.; Li, R.-H.; Fu, P.-L.; Jiang, G.-F.; Cao, K.-F. Leaf turgor loss point is correlated with drought tolerance and leaf carbon economics traits. *Tree Physiol.* **2018**, *38*, 658–663. [CrossRef] [PubMed]
52. Greenwood, S.; Ruiz-Benito, P.; Martínez-Vilalta, J.; Lloret, F.; Kitzberger, T.; Allen, C.D.; Fensham, R.; Laughlin, D.C.; Kattge, J.; Bönisch, G. Tree mortality across biomes is promoted by drought intensity, lower wood density and higher specific leaf area. *Ecol. Lett.* **2017**, *20*, 539–553. [CrossRef] [PubMed]
53. Barotto, A.J.; Monteoliva, S.; Gyenge, J.; Martinez-Meier, A.; Fernandez, M.E. Functional relationships between wood structure and vulnerability to xylem cavitation in races of Eucalyptus globulus differing in wood density. *Tree Physiol.* **2018**, *38*, 243–251. [CrossRef]
54. Laughlin, D.C.; Delzon, S.; Clearwater, M.J.; Bellingham, P.J.; McGlone, M.S.; Richardson, S.J. Climatic limits of temperate rainforest tree species are explained by xylem embolism resistance among angiosperms but not among conifers. *New Phytol.* **2020**, *226*, 727–740. [CrossRef] [PubMed]
55. Duursma, R.A.; Blackman, C.J.; Lopéz, R.; Martin-StPaul, N.K.; Cochard, H.; Medlyn, B.E. On the minimum leaf conductance: Its role in models of plant water use, and ecological and environmental controls. *New Phytol.* **2019**, *221*, 693–705. [CrossRef]

Disclaimer/Publisher's Note: The statements, opinions and data contained in all publications are solely those of the individual author(s) and contributor(s) and not of MDPI and/or the editor(s). MDPI and/or the editor(s) disclaim responsibility for any injury to people or property resulting from any ideas, methods, instructions or products referred to in the content.